# Block sparsity-based joint compressed sensing recovery of multi-channel ECG signals

*Anurag Singh* ✉, *Samarendra Dandapat*

*Electro Medical and Speech Technology Laboratory, Department of Electronics and Electrical Engineering, Indian Institute of Technology Guwahati, Guwahati-781039, India*
✉ *E-mail: anurag.singh@iitg.ernet.in*

Published in Healthcare Technology Letters; Received on 25th May 2016; Revised on 15th December 2016; Accepted on 3rd January 2017

In recent years, compressed sensing (CS) has emerged as an effective alternative to conventional wavelet based data compression techniques. This is due to its simple and energy-efficient data reduction procedure, which makes it suitable for resource-constrained wireless body area network (WBAN)-enabled electrocardiogram (ECG) telemonitoring applications. Both spatial and temporal correlations exist simultaneously in multi-channel ECG (MECG) signals. Exploitation of both types of correlations is very important in CS-based ECG telemonitoring systems for better performance. However, most of the existing CS-based works exploit either of the correlations, which results in a suboptimal performance. In this work, within a CS framework, the authors propose to exploit both types of correlations simultaneously using a sparse Bayesian learning-based approach. A spatiotemporal sparse model is employed for joint compression/reconstruction of MECG signals. Discrete wavelets transform domain block sparsity of MECG signals is exploited for simultaneous reconstruction of all the channels. Performance evaluations using Physikalisch-Technische Bundesanstalt MECG diagnostic database show a significant gain in the diagnostic reconstruction quality of the MECG signals compared with the state-of-the art techniques at reduced number of measurements. Low measurement requirement may lead to significant savings in the energy-cost of the existing CS-based WBAN systems.

**1. Introduction:** The emerging field of compressive sensing (CS) [1] is a novel sensing/sampling paradigm that enables sparse signal recovery from a small set of linear projections called *measurements*. The CS framework of data reduction consists of a simple matrix–vector multiplication, which makes signal encoding quite simple and energy efficient. There are several resource-constrained applications such as wireless body area network (WBAN)-enabled electrocardiogram (ECG) telemonitoring [2–6], which have efficiently employed the CS framework to address various challenges faced in the area, such as energy efficiency, computational complexity, memory usage and so on.

ECG signals are recorded from different locations of the body in order to capture the three-dimensional (3D) view of the human heart. In general, they are recorded in twelve channel format, which is termed as multi-channel (or multi-lead) ECG (MECG). Due to the presence of pathological information in multiple leads, cardiologists prefer MECG for detailed diagnosis [7]. The ECG signals from three channels/leads are shown in Fig. 1. It can be observed that, in addition to temporally correlated information within a single channel, different channels also have spatially correlated information. ECG signals in different channels are narrow angle projections of same electric heart vector. This generates inherent inter-channel (spatial) correlations in MECG signals in addition to intra-channel (temporal) correlations (Fig. 1). Therefore, in CS-based ECG compression techniques, spatiotemporal (spatial + temporal) correlation must be considered for optimal performance. However, most of the existing works reported in the literature have exploited either temporal correlation [2, 3, 5, 6], or spatial correlation [4, 8]. No CS-based work is reported in the literature that has exploited both types of correlations in MECG signals simultaneously. In this work, we have targeted to exploit spatiotemporal correlations during joint CS (JCS) reconstruction of different channels.

The inherent correlated structure of MECG signals becomes more visible in wavelet domain. Fig. 2 shows a joint amplitude plot of wavelet coefficients in different channels. Similar structural variations within the channel and across the channels can be clearly observed. This motivated us to explore a new CS model where this correlated structure of MECG signals can be exploited, which, in return, is expected to boost the joint recovery performance. A spatiotemporal sparse CS model [9] is employed for this purpose in place of traditional single/multiple measurement vector (SMV/MMV) CS models. The SMV/MMV CS models were used in earlier studies. A JCS-based MMV approach was proposed in [4] for power efficient joint MECG compression. Recently, we have shown that the performance of the above JCS-based approach can be enhanced substantially by emphasising the important ECG features using a weighted mixed-norm minimisation-based joint recovery algorithm [8]. The MMV-based recovery approaches although target spatial correlations, they ignore the temporal correlations within the channels itself. The SMV models, on the other hand, targets temporal correlations only as they process each ECG channel individually [2, 3, 5, 6]. The CS model employed in this work exploits the spatial as well temporal correlations simultaneously by modelling the MECG signals in a block structure form. Block structure is present in real MECG signals (Figs. 2 and 3), which can be exploited for a better JCS recovery. The proposed recovery approach adaptively learns and exploits both types of correlations while reconstructing signals from all the channels simultaneously. The significant reduction in output distortion is achieved at a reduced number of measurements (higher compression ratio) while preserving important diagnostic ECG features (P wave, QRS complex, ST segment, and T wave).

The remaining of this Letter is organised as follows: Section 2 discusses the proposed methodology. Performance evaluations and comparative study are presented in Section 3 followed by conclusions in Section 4.

**2. Methods:** CS-based data reduction approach consists of a simple matrix–vector multiplication. The resulting compressed data also called *measurements* is sent to the remote healthcare centres, where the original MECG signals are recovered back in wavelet domain using a Bayesian learning-based joint sparse recovery technique. Detailed steps are explained in the following subsections.

2.1. CS framework of multi-channel data compression

2.1.1 Problem formulation: Let us arrange the $L$ channels of $N$-dimensional MECG signals in the columns of a data matrix $\boldsymbol{X} = [\boldsymbol{x}_1, \boldsymbol{x}_2, \boldsymbol{x}_3, \ldots, \boldsymbol{x}_L] \in \mathbb{R}^{N \times L}$. Furthermore, if we use the

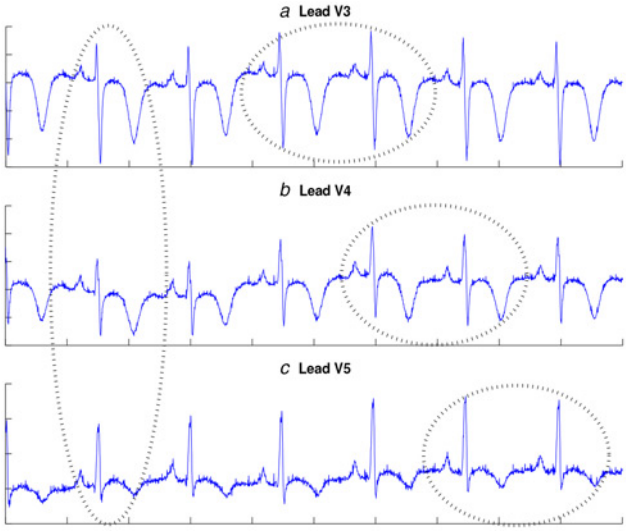


**Fig. 1** *Spatiotemporal correlation structures in MECG signals. ECG signals from three different channels/leads of dataset s0146lrem exhibiting anterior myocardial infarction are shown in a, b and c. Encircled heart beats indicate the spatially and temporally correlated information across the channels and within the channel*

same orthonormal wavelet basis $\boldsymbol{\Psi} = [\boldsymbol{\psi}_1, \boldsymbol{\psi}_2, \boldsymbol{\psi}_3, \ldots, \boldsymbol{\psi}_N]$ to represent the ECG signals from all the channels, then the joint representation is given by $\boldsymbol{X} = \boldsymbol{\Psi}\boldsymbol{A}$, where $\boldsymbol{A} = [\boldsymbol{\alpha}_1, \boldsymbol{\alpha}_2, \boldsymbol{\alpha}_3, \ldots, \boldsymbol{\alpha}_L] \in \mathbb{R}^{N\times L}$ contains the wavelet coefficient vectors of all the channels. Due to the spatiotemporal correlation among the channels, most of the diagnostically relevant information in all the ECG channels lies in low frequency wavelet subbands only. High frequency wavelet subbands are mostly noise dominated and carry very small (negligible) ECG information (Fig. 2). Therefore, $\boldsymbol{X}$ can be assumed to be having a block structure in wavelet domain, wherein few non-zero blocks only contain most of the ECG information (Fig. 3). Under this block sparsity assumption, the compressed measurement vectors corresponding to all the ECG channels in $\boldsymbol{X}$ can be obtained by

$$\boldsymbol{Y} = \boldsymbol{\Psi}\boldsymbol{X} + \boldsymbol{V} \tag{1}$$

where $\boldsymbol{\Phi}$ is a sensing matrix, $\boldsymbol{V}$ is a noise matrix, and $\boldsymbol{Y}$ is a measurement matrix of $L$ measurement vectors. Wavelet domain is used as the sparsifying transform $\boldsymbol{\Psi}$ in (1) during JCS recovery at the decoder as

$$\boldsymbol{Y} = \boldsymbol{\Phi}\boldsymbol{\Psi}\boldsymbol{A} + \boldsymbol{V} \triangleq \boldsymbol{\Theta}\boldsymbol{A} + \boldsymbol{V} \tag{2}$$

where $\boldsymbol{\Theta} = \boldsymbol{\Phi}\boldsymbol{\Psi}$. We used a binary sparse random sensing $\boldsymbol{\Phi} \in \mathbb{R}^{M\times N}$, which satisfies a modified restricted isometric property (RIP), referred to as RIP$_p$ [2]. Sparse matrices are memory-efficient and have least computational complexity, which helps minimise the energy cost of the encoder [6].

2.2. Spatiotemporal Bayesian learning-based MECG recovery: Bayesian learning-based sparse recovery algorithms are known for superior joint sparse reconstruction due to their specific feature that global minimum is always the sparsest solution unlike $\ell_1$ minimisation-based algorithms [10]. Also, they are having fewer local minima than some classic MMV algorithms. We employed a spatiotemporal sparse Bayesian learning (STSBL)-based algorithm [9] for JCS reconstruction of MECG signals. It is proposed recently for joint sparse recovery in a multi-channel scenario when signals share spatiotemporal information. STSBL model assumes that signals in ensemble possess inter-signal as well as intra-signal correlations. It processes signals ensemble in the form of groups/blocks containing spatially and temporally correlated signal samples. For MECG signals in $\boldsymbol{X}$, following block structure is assumed in wavelet domain:

$$\boldsymbol{A} = \begin{bmatrix} \boldsymbol{A}_{[1]} \\ \boldsymbol{A}_{[2]} \\ \cdot \\ \cdot \\ \cdot \\ \boldsymbol{A}_{[g]} \end{bmatrix}$$

where $\boldsymbol{A}_{[i]} \in \mathbb{R}^{d_i\times L}$ is the $i$th block of $\boldsymbol{A}$ containing $d_i$ samples from each $L$ ECG channel and $\sum_{i=1}^{g} d_i = N$. So, each block $\boldsymbol{A}_{[i]}$ now contains correlated MECG signal samples from across the channels (in rows) and from within the channels (in columns). Each block is either a non-zero block or almost a zero block. An

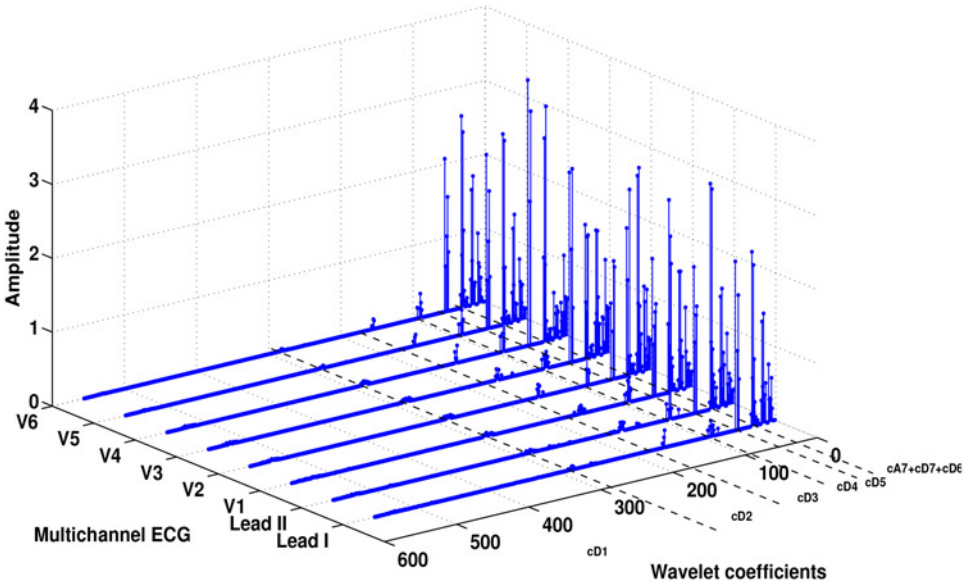


**Fig. 2** *Variation of amplitudes of wavelet coefficients in various subbands (cA7, cD7-cD1) of eight fundamental ECG channels*

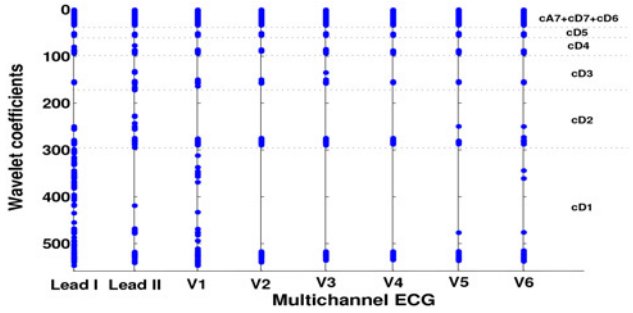


**Fig. 3** *Best K-term joint sparse approximation of MECG signals in wavelet domain. Indices of non-zero wavelet coefficients are represented by blue dots*

example of such block structure in real MECG signals is shown in Fig. 3. The STSBL model (1) assumes each block $\boldsymbol{A}_{[i]}$ having parameterised Gaussian distribution:

$$p(\text{vec}(\boldsymbol{A}_{[i]}^{\mathrm{T}});\, \gamma_i, B, C_i) = \mathcal{N}(0, (\gamma_i C_i) \otimes B), \quad i = 1, \ldots, g \tag{3}$$

where $\boldsymbol{B} \in \mathbb{R}^{\mathbb{L}\times\mathbb{L}}$ and $\boldsymbol{C} \in \mathbb{R}^{d_i \times d_i}$ are the unknown positive definite matrices capturing the inter-channel (spatial) and intra-channel (temporal) correlations in $\boldsymbol{A}_{[i]}$, respectively, and $\otimes$ is the Kronecker product. The $\gamma$ is a hyperparameter controlling the block sparsity of $\boldsymbol{A}$, i.e. a block is zero or not. The $\text{vec}(A_{[i]}^{\mathrm{T}})$ is a column vector formed by the vectorisation of 2D block $\boldsymbol{A}_{[i]}$ (by stacking its columns in a vector). Assuming blocks $\boldsymbol{A}_{[i]}$, $i = 1, 2, \ldots, g$ to be mutually independent, the distribution of matrix $\boldsymbol{A}$ is given by $p(\text{vect}(A^{\mathrm{T}}); B, \{\gamma_i, A_i\}_i) = \mathcal{N}(0, \prod \otimes B)$, where $\prod$ is a block diagonal matrix with $i$th element $\gamma_i \boldsymbol{C}_i(\forall_i)$. Similarly, noise matrix $\boldsymbol{V}$ is assumed to have similar distribution with mutually independent rows: $p(\text{vect}(V^{\mathrm{T}}), \lambda, B) = \mathcal{N}(0, \lambda I \otimes B)$, where $\lambda$ is a scalar. Using these priors, maximum a posterior (MAP) estimation of wavelet coefficient matrix $\boldsymbol{A}$ is estimated as the mean of the posterior. An expectation maximisation-based approach is adopted to estimate the parameters $\gamma$, $\boldsymbol{C}$, $\boldsymbol{B}$, and $\lambda$. More details about the parameter estimation and learning can be found in [9]. The estimated coefficient matrix $\widehat{\boldsymbol{A}}$ consists of wavelet domain MECG signals which can be transformed back into time domain using $\widehat{\boldsymbol{X}} = \boldsymbol{\Psi}^{\mathrm{T}}\widehat{\boldsymbol{A}}$.

**3. Results and discussions:** The proposed method is evaluated using MECG signals from Massachusetts Institute of Technology Beth Israel Hospital (MIT-BIH) and Physikalisch-Technische Bundesanstalt (PTB) databases [11, 12]. MIT-BIH is a 2-channel arrhythmic database carrying ECG signals from 47 subjects with sampling frequency $f_{\mathrm{s}} = 360$ Hz and 11-bit resolution. PTB is a 15-channel database carrying various diagnostic MECG signals from 290 patients sampled at $f_{\mathrm{s}} = 1$ kHz with 16-bit resolution. All the two channels of MIT-BIH database and eight fundamental channels of PTB database are used for the experiments. ECG signals are processed in the form of segments of length $N = 512$ samples [5]. Daubechies-4 (*db*4) wavelets are used as the sparsifying bases during CS recovery [8]. A random sparse binary sensing matrix $\boldsymbol{\Phi}$ with binary entries, i.e. 0s and 1s is used in the joint sensing operation [6]. The experiment is run for 50 iterations to calculate the average results with the different realisation of $\boldsymbol{\Phi}$ each time.

3.1. Performance metrics used: The performance of the proposed method is evaluated using different quality measures, such as percentage-root mean square difference (PRD), joint PRD, compression ratio (CR), and QS [4, 9, 5]. They are defined as follows:

$$\text{PRD (\%)} = \left(\frac{\|\boldsymbol{x} - \widehat{\boldsymbol{x}}\|_2}{\|\boldsymbol{x}\|_2}\right) \times 100, \tag{4}$$

$$\text{Joint PRD (\%)} = \frac{\|\boldsymbol{X} - \widehat{\boldsymbol{X}}\|_F}{\|\widehat{\boldsymbol{X}}\|_F} \times 100, \tag{5}$$

where $\boldsymbol{x}$ and $\widehat{\boldsymbol{x}}$ are the original and reconstructed ECG signals from a single channel, respectively. The data compression efficiency of the proposed method is measured using CR, which is defined in following ways:

$$\text{CR (\%)} = \frac{b_{\text{orig}} - b_{\text{comp}}}{b_{\text{comp}}} \times 100, \quad \text{CR1} = \frac{b_{\text{orig}}}{b_{\text{comp}}} \tag{6}$$

where $b_{\text{orig}}$ and $b_{\text{comp}}$ are the bits required to represent original and compressed signals, respectively. The QS defines the trade-off between CR1 and corresponding PRD and is given by: QS = CR1/PRD. However, keeping in view the less acceptability of the above defined distortion measures from clinical point of view [2], we have also calculated wavelet energy-based diagnostic distortion (WEDD) as a diagnostic distortion measure. The WEDD is defined as follows [13]:

$$\text{WEDD (\%)} = \sum_{j=1}^{S+1} w_j' \text{WPRD}_j \text{ where } w_j' = \frac{\sum_{k=1}^{N_i} w_{j,k}^2}{\sum_{i=1}^{S+1}\sum_{k=1}^{N_j} w_{i,k}^2} \tag{7}$$

where $S$ is the number of wavelet subbands or levels and $\text{WPRD}_j$ is the PRD value at the $j$th subband. A reconstructed signal is considered to be of *good* quality if the values of metrics PRD and WEDD are below 9 and 11.12%, respectively [14, 2].

3.2. Evaluation of joint reconstruction performance: First 4096 samples of the original MECG signals extracted from Lead I, aVL, and V1 of PTB dataset *s*0009 exhibiting bundle branch block (BBB) are shown in the first column of Fig. 4. The corresponding reconstructed signals using the proposed approach at CR = 74.32% are shown in the second column of the figure. It is evident from the reconstructed waveforms that the diagnostic information of the BBB signals such as QRS complex duration, secondary R-wave ($\text{RSr}'$ complex) and slurred S-wave (encircled and indicated by arrows) are well preserved without any noticeable alteration. For noisy signals like Lead I and aVL signals, the noise level gets reduced in the reconstructed signals without any loss of aforementioned clinical features. The corresponding PRD and WEDD values in three leads of Fig. 4 are found to be 0.510, 0.883, 1.851%, and 2.59, 3.76, 6.26%, respectively. Slightly higher PRD/WEDD value for Lead V1 is due to the marginal loss in amplitudes of R-waves in the reconstructed signal, which is also reflected in the error plot. Recovery results for specific pathological cases where normal sinus rhythm is not present, such as premature ventricular contraction (PVC) and ventricular fibrillation (VF), are also evaluated. Reconstruction result (overlapped with the original signal) in case of VF recovery is shown in Fig. 5 for data record 419 of MIT-BIH Malignant Ventricular Arrhythmia Database (VFDB) at CR = 73.82%. It is observed that in the case of PVC, diagnostic ECG features, i.e. PVC beats are well preserved except a nominal loss in their positive amplitudes. However, in the case of VF, some distortions are observed in the reconstructed waveforms, especially at the edges/notches of the fibrillatory waves (pointed out by the arrows in Fig. 5), resulting in relatively higher PRD value (= 9.22%). This may be due fibrillatory nature of ECG, which makes it almost non-sparse and

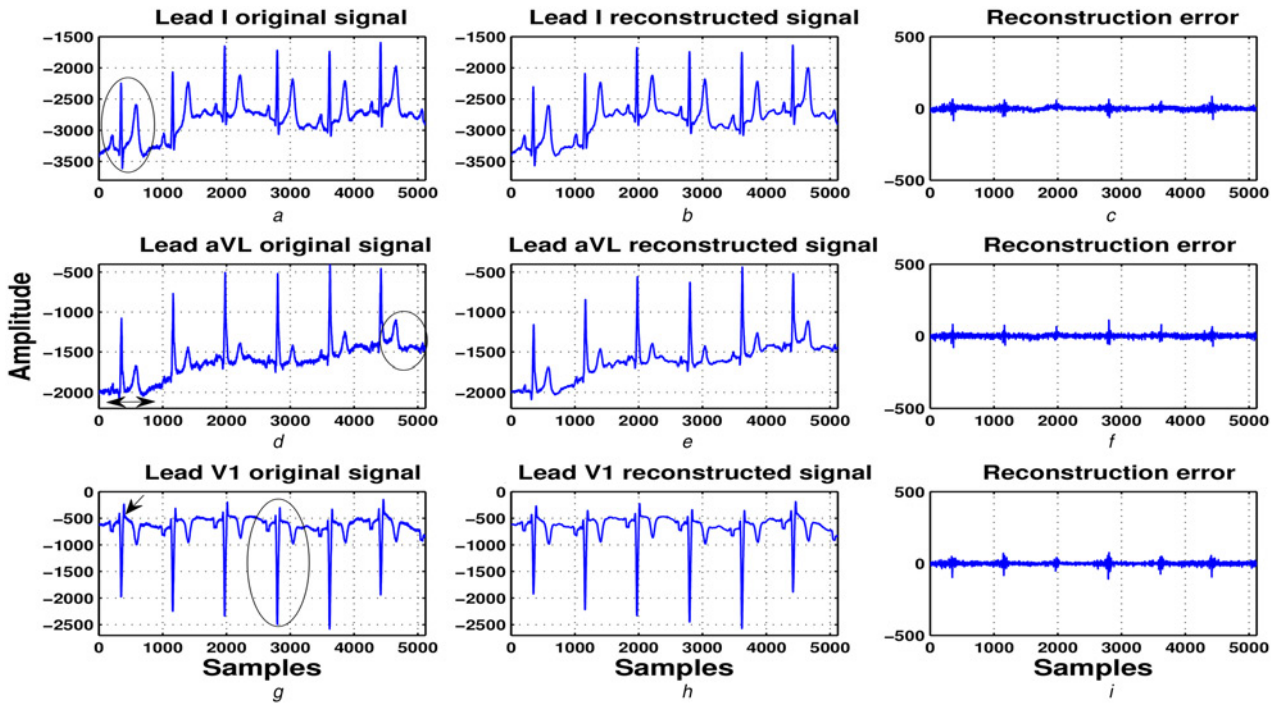


**Fig. 4** *Signal reconstruction quality of the MECG signals taken from PTB dataset s0008rem exhibiting BBB using the proposed approach. Original signals from channels I, aVL, and V1 are shown in (a), (d), (g), and the corresponding recovered signals at CR = 74.32% are depicted in (b), (e), (h). Reconstruction error is shown in plots (c), (f), (i). Diagnostic features are encircled and indicated by arrows*

*a* Lead I original signal
*b* Lead I reconstructed signal
*c* Reconstruction error
*d* Lead aVL original signal
*e* Lead aVL reconstructed signal
*f* Reconstruction error
*g* Lead V1 original signal
*h* Lead V1 reconstructed signal
*i* Reconstruction error

hence challenging to recover. It can be noted that STSBL-based JCS compression/recovery is performed directly on raw MECG signals without any pre-processing steps. This can be observed in Fig. 4, where the original signals contain different types of noise such as baseline wandering, power-line noise and so on. In such a noisy scenario also, the proposed method works satisfactorily. This establishes the ability of the proposed approach to perform equally well in noisy scenarios also without the need of any pre-processing/noise cancellation module. Pre-processing steps such as filtering, peak detection, dynamical thresholding and so on are not favoured in resource-constrained WBAN applications in order to reduce circuitry complexity and hence energy cost [9].

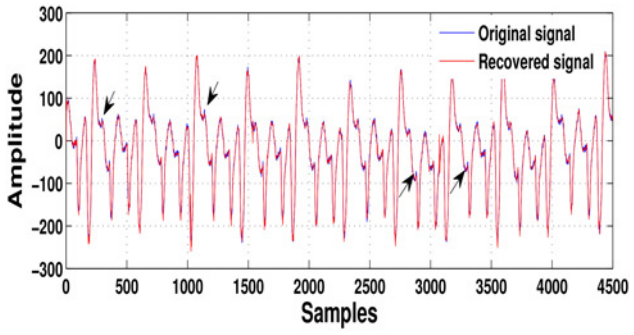


**Fig. 5** *Reconstruction results of the proposed method for ECG signals from data record 419 of VFDB database exhibiting VF at CR = 73.82%. Arrows indicate the points of distortion in the reconstructed signals*

STSBL algorithm exploits both types of correlations present in the MECG signals that results superior reconstruction even at the low number of measurements ($M$) or at higher CR. Average joint PRD variation across the PTB database with $M$ is shown in Fig. 6. It can be observed that reconstruction error in terms of PRD decreases as more CS measurements are used for the recovery and vice-versa. For noisy MECG signals, we used a little higher value or hyperparameter $\gamma(=0.01)$ in STSBL algorithm. As the MECG signals are repetitive in nature, we used fixed block size $(d_i, i = 1, \ldots, g)$ over the length of the signal. Its value is

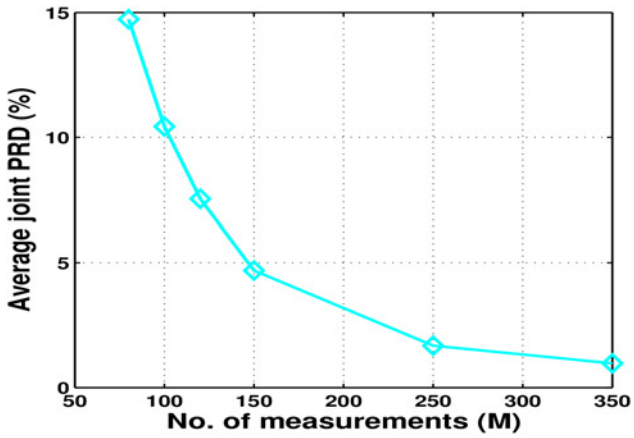


**Fig. 6** *Average joint PRD variation with the number of measurements*

**Table 1** Average PRD values with standard deviations in different leads of ECG signals from normal and different pathological classes of PTB database at number of measurements, $M = 120$. Average PRD is calculated over all the datasets of a particular class in the PTB database

| Pathological classes | No. of datasets | PRD value in different ECG channels | | | | | | | |
|---|---|---|---|---|---|---|---|---|---|
| | | Lead I | Lead II | V1 | V2 | V3 | V4 | V5 | V6 |
| Healthy control | 52 | 5.47 ± 4.68 | 4.63 ± 2.85 | 5.31 ± 3.24 | 4.74 ± 3 | 5.77 ± 3.42 | 7.03 ± 3.77 | 7.84 ± 2.54 | 6.75 ± 2.45 |
| Myocardial infarction | 148 | 9.49 ± 7.43 | 6.76 ± 6.73 | 6.39 ± 4.27 | 5.80 ± 3.32 | 5.20 ± 3.11 | 6.52 ± 3.64 | 8.12 ± 5.02 | 8.45 ± 5.43 |
| Hypertrophy | 7 | 6.82 ± 3.32 | 4.60 ± 4.99 | 3.76 ± 2.18 | 3.62 ± 1.60 | 4.29 ± 2.06 | 5.58 ± 2.66 | 5.73 ± 1.99 | 4.71 ± 2.80 |
| Bundle branch block | 15 | 3.29 ± 3.41 | 3.90 ± 3.99 | 4.17 ± 3.83 | 3.59 ± 2.21 | 3.96 ± 2.81 | 4.97 ± 2.80 | 3.78 ± 2.65 | 3.67 ± 2.31 |

chosen experimentally and taken as $d_1 = d_2 = \cdots = d_g = 25$ in all the simulations.

Average performance results across all the datasets of PTB database are also calculated. To analyse the class specific performance variance of the proposed method, it is evaluated over four major classes of pathologies present in the PTB database, such as HC, myocardial infarction (MI), hypertrophy (HP), and BBB. Average PRD values with standard deviations calculated across all the datasets available in a particular pathological class are given in Table 1 at $M = 120$. Most of the PRD values in each class and in each channel fall in good category reconstruction (PRD < 9%) even after taking standard deviation into account. In the case of MI and few leads of HC, high standard deviation is observed, which may be due to the large number of patient's data available there. However, the overall average PRD over 222 datasets is still found to be in good quality signal reconstruction category (Table 1). Variance of the results obtained across different datasets is also studied. Average WEDD variation for Lead II in all the pathological and normal data records of PTB database is shown in the form of box plots in Fig. 7. The edges of the box plots are 25th and 75th percentiles with central line as median. The extreme values in individual box plot depict the minimum and maximum WEDD values obtained at a particular value of CR for different datasets. Variations are observed in the WEDD values for different datasets at the same CR level. This is because normal and arrhythmic data records taken for evaluation consist of MECG signals with different morphological characteristics. This leads to varying joint sparsity profile and hence varying performances as reflected in Fig. 7. As we start compressing the data further, the WEDD values start increasing and vice-versa.

To verify the diagnostic information preservation, we also calculated a subjective quality measure called mean opinion score (MOS) [14]. The visual distortions in the recovered signals are quantifies by the qualitative distortion measure, i.e. MOS. The subjective evaluation to calculate MOS is carried out with different evaluators that include 5 doctors of IIT Guwahati hospital and 14 research scholars/project engineers working in biomedical area. Different diagnostic ECG features of different pathological cases studied in this work are evaluated in a semi-blind test where the evaluators are asked to find the waveform similarity given the original and reconstructed ECG signals. Following quality rating is used for this evaluation: 1 (bad), 2 (almost tolerable), 3 (tolerable), 4 (good), and 5 (excellent) [14]. The average MOS error in percentage for different pathological features of ECG signals for different pathological classes is given in Table 2. According to standard MOS rating [14], all the clinically important ECG features either fall into the *very good* (0 < MOS < 15%) or *good* (15% < MOS < 35%) quality group of signal reconstruction. Moreover, MOS error for overall ECG signal is also calculated and it is found that ECG with BBB is having minimum MOS error of 8.89%.

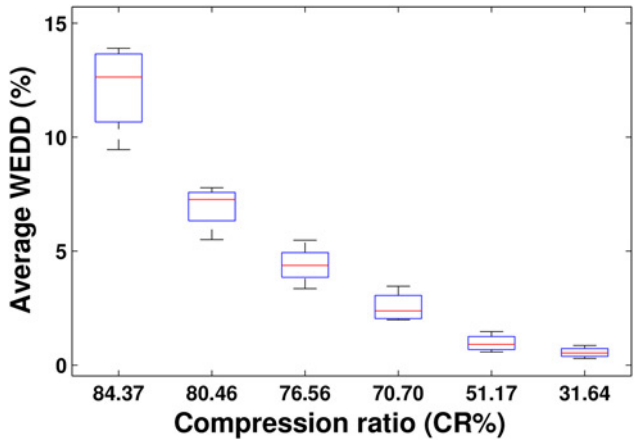


**Fig. 7** *Boxplot showing the variation of PRD values of different datasets of PTB database at different CR values*

3.3. Comparative study: The performance of the proposed method is compared with two types of CS-based works reported in the literature: one that targets temporal correlations and deals with single channel ECG signals individually [5, 6], and second types include those algorithms which exploit spatial correlations and deal multiple ECG channels simultaneously [4, 8]. The comparison results in terms of reconstruction distortion at almost same *CR* values or *M* values (as reported in the respective works) are given in Table 3. The quantitative results suggest that exploiting both types of correlations simultaneously can substantially improve the recovery results of CS-based works. In [5, 6], weighted $l_1$ (WLM) and iterative hard thresholding (MMB-IHT) algorithms were used to individually compress and reconstruct each ECG channel of MIT-BIH database. However, the spatially correlated information that exists between different channels was ignored in the above works. The proposed work processes multiple channels simultaneously and thus exploits this

**Table 2** MOS error (in %) in different types of ECG signals

| ECG features | BBB | HC | HP | MI | PVC | VF |
|---|---|---|---|---|---|---|
| P wave | 8.57 | 17.14 | 17.28 | 17.14 | 21.42 | – |
| Q wave | – | – | – | 15.71 | – | – |
| QRS complex | 7.85 | 10 | 7 | 17.14 | 14.28 | – |
| QRS duration | 8.28 | – | 7.14 | – | – | – |
| ST segment | 9 | 14.28 | 10.46 | 15.71 | 17.14 | – |
| T wave | 13.14 | 12.85 | 8.15 | 10.76 | 12.85 | – |
| RSr′ complex | 7 | – | – | – | – | – |
| Slurred S wave | 8.42 | – | – | – | – | – |
| PVC beat 1 | – | – | – | – | 12.85 | – |
| PVC beat 2 | – | – | – | – | 12.85 | – |
| VF waves | – | – | – | – | – | 14.28 |
| Overall ECG signal | 8.89 | 13.5 | 10 | 15.29 | 15.23 | 14.28 |




doi: 10.1049/htl.2016.0049

**Table 3** Performance comparison table

| Techniques | Distortion metrics | | CR(M) | Correlation type | Database |
|---|---|---|---|---|---|
| **Proposed** | PRD | 2.15 | 6.58 | spatiotemporal | MIT-BIH ($f_s = 360$ Hz) |
| | QS | 3.06 | | | |
| | WEDD | 1.13 | | | |
| MMB-IHT [5] | PRD | 3.74 | 6.4 | temporal | |
| | QS | 1.71 | | | |
| **Proposed** | PRD | 1.67 | 192 | spatiotemporal | |
| WLM [6] | PRD | 3.64 | 192 | temporal | |
| **Proposed** | PRD | 4.68 | 73.3% | spatiotemporal | PTB ($f_s = 1$ kHz) |
| | WEDD | 3.61 | | | |
| JCS [4] | PRD | 9.00 | 72.7% | spatial | |
| WMNM [8] | PRD | 5.5 | 73.4% | spatial | |
| PWMNM [15] | PRD | 3.3 | 73.9% | spatial | |

correlation during JCS reconstruction, which results in lower PRD and higher QS values at reported CR1 = 6.4 and $M = 192$. In another JCS-based work [4], the shared information across the channels was utilised by a row-sparse modelling of MECG signals. Here, the authors used a mixed norm-based convex optimisation algorithm for joint reconstruction of all the channels simultaneously. Recently, we proposed a weighted mixed norm minimisation (WMNM)-based JCS recovery algorithm to emphasise the important ECG features through coefficient-based weighting approach. The WMNM technique improves the recovery performance and substantially reduces the PRD value from 9% in the case of JCS to 5.5%. However, in row-sparse modelling, single sample from each channel falling within a row are emphasised and thus overlooking the temporally correlated samples within a channel. The STSBL algorithm employed in the proposed work targets inherited spatiotemporal correlations of MECG signals simultaneously by modelling different channels into block structure form. This helps it outperform other techniques in the form of reduced distortion levels at same CR (or $M$) values. We also compared the recovery results of STSBL with our latest work [15]. In this work, we attempted to exploit the multi-scale signal information through a weighting approach and proposed a prior weighted mixed-norm minimisation (PWMNM) algorithm for JCS recovery. It is found that PRD value for STSBL is relatively higher than subband weighting-based PWMNM algorithm. Though PWMNM is also based on spatial correlation only, it exploits diagnostically important multi-scale information additionally, through the subband-based weighting approach. On the other hand, STSBL only leverages block-sparsity and does not utilise any other additional prior signal information. In this way, PWMNM becomes more signal-adaptive than STSBL, which might help it to emphasise clinically relevant ECG features more precisely during JCS recovery and results in lower PRD value compared with STSBL. Though WMNM also uses coefficient-based weighting, its weighting scheme is not as effective as subband-based weighting PWMNM, and hence produces higher PRD value. Despite having little higher PRD value than PWMNM, STSBL approach can be advantageous in many ways: (i) it is significantly faster (0.96 s) than the other algorithms, such as WMNM (12.78 s), JCS (3.81 s) and PWMNM (3.72 s) on the same platform, (ii) its computational time does not scale with the number of channels and remains almost stable for 2 channels (0.89 s), 8 channels (0.96 s), and 12 channels (0.98 s) ECG signal, (iii) the STSBL algorithm is capable of signal encoding efficiently even with the simplest sensing matrix (with only $d = 2$ number of 1s in each column), which enables faster data encoding, lower power consumption, and simplified circuit design, and (iv) furthermore, STSBL can operate directly on raw MECG data (Fig. 4) without requirement of any pre-processing steps, which makes it more energy efficient.

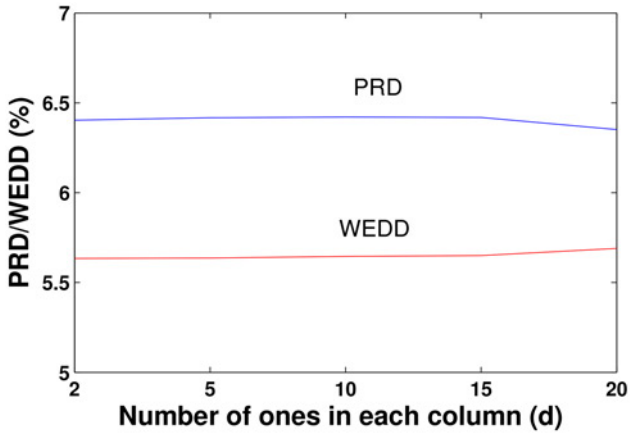


**Fig. 8** *Output distortions variation with number of 1 s in each column of sensing matrix* $\boldsymbol{\Phi}$

3.4. Computational complexity and power efficiency: From the power saving point of view in practical applications, a random sparse binary sensing matrix is employed during the entire encoding process with entries of 0s and 1s [6]. Sparse binary matrices replace the multiplication operations with simple additions at the encoder. This reduces the number of on-chip computations and cuts down the computational cost during the signal sensing. This improves the power efficiency as compared with the cases where sensing matrix $\Phi$ has non-binary entries [2, 3].

The number of 1s ($d$) in each column of sensing matrix directly corresponds to the computations involved in the encoding process. The low number of 1s is highly desirable from the power saving perspective. So, the performance of the proposed STSBL-based joint recovery algorithm is also analysed with respect to $d$. The reconstruction errors in terms of PRD and WEDD are plotted in Fig. 8 at different values of $d$. It can be observed that the distortions remain almost invariant with the change in values of $d$. This is a very important characteristic of Bayesian learning-based approach. We used $d = 2$ in all experiments. So, STSBL helps save more than 90% energy in the encoding process compared with JMCS [4] which uses $d = 35$ number of 1s in each column.

**4. Conclusion:** A Bayesian learning-based sparse recovery approach was proposed to exploit spatial and temporal correlations simultaneously in CS-based WBAN-enabled MECG telemonitoring systems. Efficient exploitation of spatiotemporal correlations substantially improved the recovery performance of CS at low number of measurements. Low measurement

requirement reduces the on-chip computations and can eventually lead to reduction in the volume of the data to be transmitted over power hungry wireless links. Also, the number of computations was made to reduce further at the encoder by employing a sparse binary sensing matrix with only two 1s in each column. Therefore, the proposed method is able to achieve good quality of signal reconstruction with reduced computational load at the encoder, which may lead to significant power savings in CS-based ECG telemonitoring applications.

**5. Funding and Declaration of Interests:** Conflict of interest: none declared.

## 6 References

[1] Candes E.J., Wakin M.B.: 'An introduction to compressive sampling', *IEEE Signal Process. Mag.*, 2008, **25**, (2), pp. 21–30

[2] Mamaghanian H., Khaled N., Atienza D., *ET AL.*: 'Compressed sensing for real-time energy-efficient ECG compression on wireless body sensor nodes', *IEEE Trans. Biomed. Eng.*, 2011, **58**, (9), pp. 2456–2466

[3] Polania L.F., Carrillo R.E., Blanco-Velasco M., *ET AL.*: 'Compressed sensing based method for ECG compression'. 2011 IEEE Int. Conf. on Acoustics, Speech and Signal Processing (ICASSP), Prague, 2011, pp. 761–764

[4] Mamaghanian H., Ansaloni G., Atienza D., *ET AL.*: 'Power-efficient joint compressed sensing of multi-lead ECG signals'. 2014 IEEE Int. Conf. on Acoustics, Speech and Signal Processing (ICASSP), Florence, 2014, pp. 4409–4412

[5] Polania L.F., Carrillo R.E., Blanco-Velasco M., *ET AL.*: 'Exploiting prior knowledge in compressed sensing wireless ECG systems', *IEEE J. Biomed. Health Inform.*, 2015, **19**, (2), pp. 508–519

[6] Zhang J., Gu Z., Yu Z.L., *ET AL.*: 'Energy-efficient ECG compression on wireless biosensors via minimal coherence sensing and weighted $\ell_1$ minimization reconstruction', *IEEE J. Biomed. Health Inform.*, 2015, **19**, (2), pp. 520–528

[7] Surawich B., Knilans T.: 'Chou's electrocardiography in clinical practice' (Elsevier, 2008, 6th edn.)

[8] Singh A., Dandapat S.: 'Weighted mixed-norm minimization based joint compressed sensing recovery of multi-channel electrocardiogram signals', *Comput. Electr. Eng.*, 2016, **53**, pp. 203–218

[9] Zhang Z., Jung T.P., Makeig S., *ET AL.*: 'Spatiotemporal sparse Bayesian learning with applications to compressed sensing of multichannel physiological signals', *IEEE Trans. Neural Syst. Rehabil. Eng.*, 2014, **22**, (6), pp. 1186–1197

[10] Zhang Z., Rao B.D.: 'Sparse signal recovery with temporally correlated source vectors using sparse Bayesian learning', *IEEE J. Sel. Top. Signal Process.*, 2011, **5**, (5), pp. 912–926

[11] Goldberger A.L., Amaral L.A.N., Glass L., *ET AL.*: 'Physiobank, physiotoolkit, and physionet: components of a new research resource for complex physiologic signals', *Circulation*, 2000, **101**, (23), pp. e215–e220 [Circulation Electronic Pages; http://circ.ahajournals.org/cgi/content/full/101/23/e215]

[12] www.physionet.org

[13] Manikandan M.S., Dandapat S.: 'Wavelet energy based diagnostic distortion measure for ECG', *Biomed. Signal Proc. Control*, 2007, **2**, (2), pp. 80–96

[14] Zigel Y., Cohen A., Katz A.: 'The weighted diagnostic distortion (WDD) measure for ECG signal compression', *IEEE Trans. Biomed. Eng.*, 2000, **47**, (11), pp. 1422–1430

[15] Singh A., Dandapat S.: 'Exploiting multi-scale signal information in joint compressed sensing recovery of multi-channel ECG signals', *Biomed. Signal Proc. Control*, 2016, **29**, pp. 53–66